Nonlinear Dyn (2022) 109:1005–1017
https://doi.org/10.1007/s11071-022-07441-3

ORIGINAL PAPER

Dynamic behavior and stability analysis of nonlinear modes in the fourth-order generalized Ginzburg–Landau model with near $\mathcal{PT}$-symmetric potentials

Jia-Rui Zhang · Jia-Qi Zhang · Zhao-Lin Zheng · Da Lin · Yu-Jia Shen

Received: 28 December 2021 / Accepted: 7 April 2022 / Published online: 5 May 2022

Abstract We investigate the fourth-order generalized Ginzburg–Landau equation and the nonlinear modes modulated by $\mathcal{PT}$-symmetric potentials. By means of Hirota method, we obtained the bilinear form of the equation and further derived the analytic soliton solution. Dynamic behaviors of the solitons under the modulation of near $\mathcal{PT}$-symmetric potentials were studied by numerical simulation: The nonlinear modes tend to be unstable when the potential is closer to conventional $\mathcal{PT}$-symmetric potential, and the amplitude of the nonlinear modes oscillates periodically when the imaginary part of the $\mathcal{PT}$-symmetric potentials is sufficiently large. Moreover, we obtained new nonlinear modes that are different from the above analytic soliton solutions by numerical excitation and tested their stability. These new findings of nonlinear modes in the generalized Ginzburg–Landau model can be potentially applied to hydrodynamics, optics and matter waves in Bose–Einstein condensates.

Keywords Generalized Ginzburg–Landau equation · Near $\mathcal{PT}$-symmetric potential · Stable nonlinear mode · Soliton and peakon solutions

Mathematics Subject Classification 37K40 · 35C08

J.-R. Zhang · Z.-L. Zheng · D. Lin · Y.-J. Shen (✉)
College of Science, China Agricultural University, Beijing 100083, China
e-mail: yjshen2018@cau.edu.cn

J.-Q. Zhang
College of Engineering, China Agricultural University, Beijing 100083, China

1 Introduction

Ginzburg–Landau models have attracted the attention of researchers recently because they are the universal wave equations that govern many nonlinear phenomena such as hydrodynamics, optics and matter waves in Bose–Einstein condensates [1–6]. The conventional Ginzburg–Landau equation (GLE) [7–9]

$$iu_t + pu_{xx} + q|u|^2u = i\gamma u \tag{1}$$

is the dissipative extension of the conservative nonlinear Schrödinger equation and has also been widely used in superfluidity, plasmas, liquid crystals, strings in the field theory, quantum field theory, etc. [10–12]. With the development of symbolic computation and soliton theory, various types of soliton solutions of GLE are analyzed in detail, including multi-peak solitons [13], exploding solitons [14], two-dimensional vortical solitons [15], lattice solitons [16] and peakons. Although the higher-order GLEs have been investigated, nonlinear modes of them have rarely been analyzed so far. Therefore, the main purpose of this paper is to study the generalization of GLE with fourth-order nonlinear dispersion by means of analytical and numerical methods.

We will investigate the fourth-order generalized GLE:

$$iu_t + \alpha(x)u_{xx} + \beta(x,t)|u|^2u + \gamma(x,t)u + \sigma(t)u_{xxxx} + \zeta(t)u_{xx}|u|^2 + \xi(t)u|u|^2_{xx} + \rho(t)u|u|^4 + \eta(t)u_x = 0, \tag{2}$$

with $\alpha = \alpha_1 + i\alpha_2$, $\beta = \beta_1 + i\beta_2$, $\gamma = V + iW$, $\sigma = \sigma_1 + i\sigma_2$, $\zeta = \zeta_1 + i\zeta_2$, $\xi = \xi_1 + i\xi_2$, $\rho = \rho_1 + i\rho_2$, $\eta = i\eta_1$, where V, α_i $(i = 1, 2)$ are real functions of x; η_1, σ_i, ζ_i, ξ_i, ρ_i $(i = 1, 2)$ are real functions of t; and W, β_i $(i = 1, 2)$ are real functions of x and t. To indicate the linear gain–loss coefficient, we introduce the complex potential $V + iW$ [10].

Equation (2) can be applied to describe the propagation of light in an active dispersive medium [17]. In this case, u is the complex envelope of the electric field, x denotes the propagation distance, and t is the retarded time. α_1 is the group velocity dispersion coefficient, and α_2 describes the spectral filtering or linear parabolic gain [14]. β_1 is the Kerr nonlinearity coefficient, and β_2 accounts for the nonlinear gain–loss processes [10]. ρ_1 is the parameter of the quintic nonlinearity and represents a higher-order correction to the nonlinear amplification/absorption, and ρ_2 characterizes the saturation of the nonlinear gain and it is a possible higher-order correction term to the intensity-dependent refractive index [17]. σ represents the effect due to discreteness and higher-order magnetic interactions [18]. V is related to the refractive index waveguide, and W characterizes the amplification (gain) or absorption (loss) of the light beam in the optical material [10,19].

There are three special cases of Eq. (2) that should be mentioned:

(i) When α, β, γ are constants and the other coefficients are zero, Eq. (2) degenerates to Eq. (1). The stable optical soliton can be obtained by regulating the group velocity dispersion and nonlinear gain–loss coefficient [20]. Moreover, many kinds of analytical coherent structure solutions to this equation have been studied [21].

(ii) When $\alpha = \beta = 1$, $\gamma(x,t) = V(x) + iW(x)$ and the other coefficients are zero, Eq. (2) can be reduced to

$$iu_t + u_{xx} + [V(x) + iW(x)]u + |u|^2u = 0, \tag{3}$$

in which the beam evolution is governed by the normalized nonlinear Schrödinger-like equation. It can be used to describe the propagation of the optical soliton in a self-focusing Kerr nonlinear $\mathcal{PT}$-symmetric potential [3].

(iii) When α, β are complex constants, $\gamma(x,t) = V(x) + iW(x)$ and the other coefficients are zero, Eq. (2) can be reduced to

$$iu_t + (\alpha_1 + i\alpha_2)u_{xx} + [V(x) + iW(x)]u + (\beta_1 + i\beta_2)|u|^2u = 0, \tag{4}$$

which can describe the spatial beam transmission in a cubic-nonlinear optical medium described by the complex Ginzburg–Landau equation with complex potentials. Moreover, the stability of soliton has been analyzed via numerical simulation [10].

Initiated by Bender and his coworker in 1998 [22–24], $\mathcal{PT}$ symmetry and its applications have become hot topics in physics research in optical experiments [25–33]. In recent years, there has been tremendous interest in investigating one- and multi-dimensional solitons and their stability in all stripes of optical potentials [3,27,29,34,35]. In the $\mathcal{PT}$-symmetric cases, the spatial profiles of the refractive index and the gain–loss are even and odd functions, respectively [3]. Due to some special purposes or uncontrollable elements, however, the complex potentials can be asymmetric in several realistic photonics applications and it has been proved that waveguides with an asymmetric distribution in the transverse direction of gain and loss can have stable modes [36–38]. In addition, stable solitons in the nonlinear Schrödinger equation with certain non-$\mathcal{PT}$-symmetric potentials have also been reported in recent research [4,38–43]. So it is necessary to extend the studies on the formation and dynamics of nonlinear modes in non-$\mathcal{PT}$-symmetric complex potentials [44,45]. The non-$\mathcal{PT}$-symmetric potentials can be bifurcated out from the $\mathcal{PT}$-symmetric potential by regulating the related potential parameters, which are called the near $\mathcal{PT}$-symmetric potentials [10,35]. Our aim is to investigate Eq. (2) with the near $\mathcal{PT}$-symmetric potentials and obtain stable nonlinear modes.

In Sect. 2, under some constraints of the constant and variable coefficients that will be derived, Eq. (2) will be linearized. Based on the bilinear forms, one-soliton solutions will be derived. In Sect. 3, we will

perform numerical simulation of Eq. (2) with near $\mathcal{PT}$-symmetric potentials in two cases, corresponding to the near $\mathcal{PT}$-symmetric Scarf-II and δ-signum potentials, respectively. Then, we consider excitations of solitons via making the parameters rely on the propagation distance t. In Sect. 4, results will be summarized.

2 Analytical soliton solutions of Eq. (2)

To get the bilinear forms of Eq. (2), we will present the following constraints on the variable coefficients:

$$\begin{aligned}\alpha(x)\beta(x,t)\zeta(t) &= 6\beta^2(x,t)\sigma(t)\\ &= 6\alpha(x)\beta(x,t)\xi(t) = 2\alpha^2(x)\rho(t).\end{aligned} \tag{5}$$

Via the dependent-variable transformation

$$u(x,t) = \frac{g(x,t)}{f(x,t)}, \tag{6}$$

with the real f and complex g, we can derive the bilinear forms of Eq. (2):

$$\begin{aligned}&iD_t g\cdot f + \alpha(x)D_x^2 g\cdot f + \gamma(x,t)g\cdot f\\ &\quad + \sigma(t)D_x^4 g\cdot f + \eta(t)D_x g\cdot f = 0,\\ &\alpha(x)D_x^2 f\cdot f - \beta(x,t)|g|^2 = 0.\end{aligned} \tag{7}$$

Through Hirota bilinear method, we introduce the bilinear operator D defined as [46]

$$\begin{aligned}&D_x^m D_t^n a(x,t)\cdot b(x,t)\\ &\quad = \frac{\partial^m}{\partial y^m}\frac{\partial^n}{\partial s^n}a(x+y,t+s)b(x-y,t-s)\Big|_{y=0,s=0},\end{aligned} \tag{8}$$

where m, n are positive integers, a, b are functions of x and t, and y stands for the small increment.

Then, we expand g and f in power series of a small parameter ϵ as

$$\begin{aligned}g &= \epsilon g_1 + \epsilon^3 g_3 + \epsilon^5 g_5 + \cdots,\\ f &= 1 + \epsilon^2 f_2 + \epsilon^4 f_4 + \epsilon^6 f_6 + \cdots,\end{aligned} \tag{9}$$

where $g_m (m = 1, 3, 5, \cdots)$, $f_n (n = 2, 4, 6, \cdots)$ are functions of x and t to be determined.

2.1 The case of constant coefficients

In this section, we assume the coefficients of Eq. (2) are constant and set

$$\begin{aligned}g_1 &= e^{k_1 x+(\omega_1+i\omega_2)t+\theta_1},\\ f_2 &= A_1 e^{2k_1 x+2\omega_1 t+2\theta_1},\end{aligned} \tag{10}$$

where k_1, A_1, ω_i $(i = 1, 2)$ are nonzero constants. Let $\beta_1 = c_0\alpha_1$, $\beta_2 = c_0\alpha_2$, $c_0 = 8A_1k_1^2$, and we can derive the constraint relation of other parameters:

$$\begin{aligned}\omega_1 &= -k_1^2\alpha_2 - W - k_1\eta_1 - k_1^4\sigma_2,\\ \omega_2 &= k_1^2\alpha_1 + V + k_1^4\sigma_1,\\ W &= -k_1^4\sigma_2 - k_1^2\alpha_2.\end{aligned} \tag{11}$$

Without loss of generality, we set $\epsilon = 1$. Thus, the expression of single soliton solution can be written as

$$u = \frac{g_1}{1+f_2}. \tag{12}$$

In Fig. 1, the propagation of the soliton along the distance x is illustrated. The velocity and direction of solitonic propagation phase will be changed if we choose different values of η_1. Moreover, the amplitude of the soliton is determined by k_1.

2.2 The case of various coefficients

Next, we will consider the situation that the coefficients of Eq. (2) are functions of x, t and assume

$$\begin{aligned}g_1 &= A_1(t)\,\mathrm{e}^{k_1 x+\omega_1(t)+i\omega_2(t)},\\ f_2 &= A_2(t)\,\mathrm{e}^{2k_1 x+2\omega_1(t)}.\end{aligned} \tag{13}$$

Then, we separate $W(x,t)$ into two parts by $W(x,t) = W_1(x) + W_2(t)$ and take $\beta_1(x,t) = 2c_0(t)\alpha_1(x)$, $\beta_2(x,t) = 2c_0(t)\alpha_2(x)$.

The expressions of variable coefficients can be obtained

$$\begin{aligned}A_1(t) &= \mathrm{e}^{\int -W_2(t)dt},\\ A_2(t) &= \frac{A_1^2(t)c_0(t)}{4k_1^2},\\ \omega_1(t) &= \int -k_1(\eta_1(t) + k_1^3\sigma_2(t))dt,\end{aligned}$$

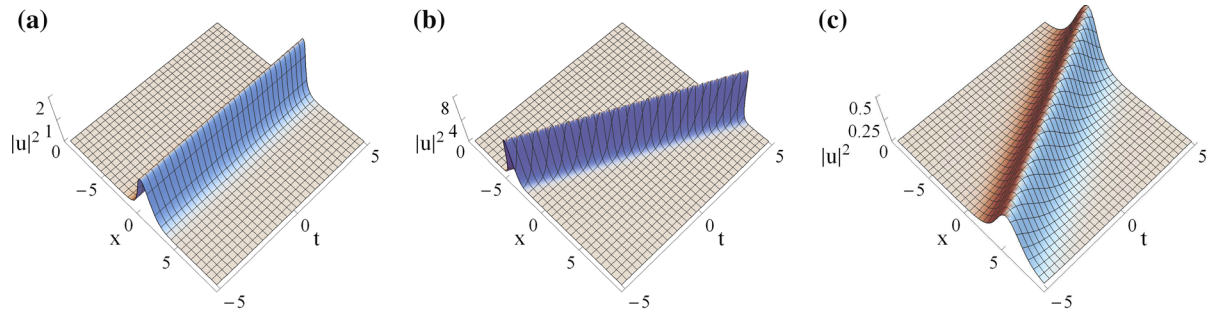

Fig. 1 Parameters are chosen as: **a** $k_1 = 1, \alpha_2 = 1, c_0 = 1, \eta_1 = 0, \theta_1 = 0$. **b** and **c** have two different parameters from **a**, with $k_1 = 2$, $\eta_1 = 1$ in **b** and $k_1 = 0.5$, $\eta_1 = -1$ in **c**

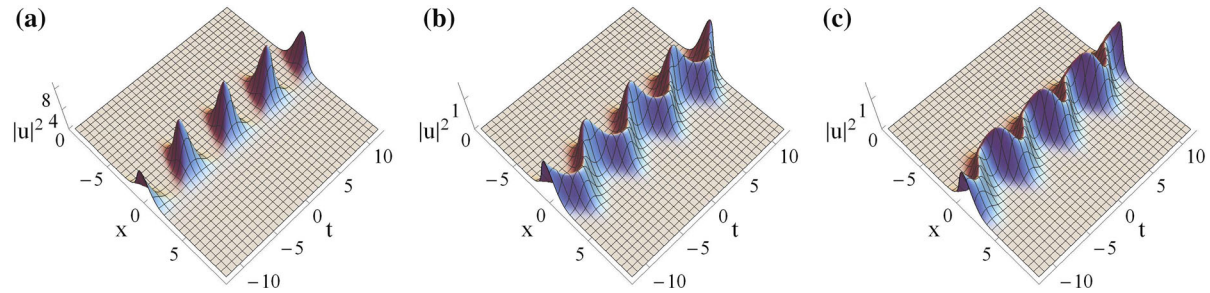

Fig. 2 Parameters are chosen as: $k_1 = 1, c_1 = 1$, with **a** $W_2(t) = 0.1\sin(2t), \eta_1(t) = \sin(t), \sigma_2(t) = \sin(t)$, with **b** $W_2(t) = 0.1\sin(2t)$, $\eta_1(t) = \sin(t)$, with $\sigma_2(t) = 0.1\sin(t)$, with **c** $W_2(t) = 0.1\sin(2t)$, $\eta_1(t) = \cos(t)$, $\sigma_2(t) = 0.1\sin(t)$

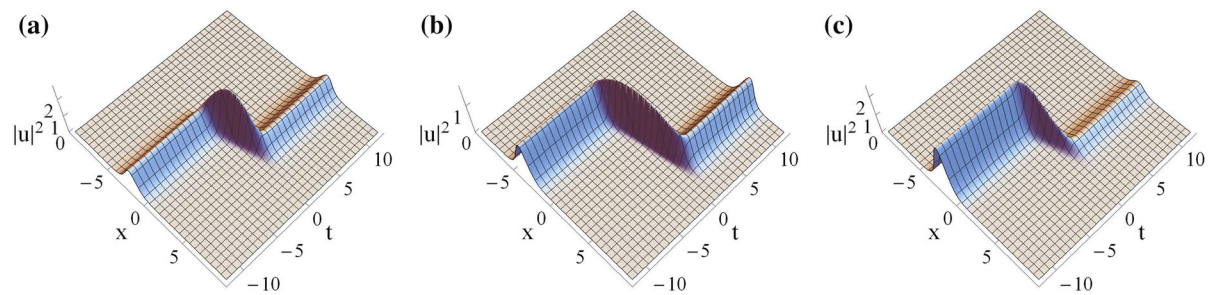

Fig. 3 Parameters are chosen as: $k_1 = 1, c_1 = 1$, with (a) $a = 1, b = 3, c = 0.1$, with (b) $a = 0.5, b = 5, c = 0.1$, with (c) $a = 0.5$, $b = 3, c = 0.5$

$$\omega_2(t) = \int k_1^4 \sigma_1(t)dt,$$
$$c_0(t) = c_1\, \mathrm{e}^{\int 2(W_2(t)+k_1^4\sigma_2(t))dt}, \tag{14}$$

where c_1, k_1 are constants, $V(x) = -k_1^2\alpha_1(x)$, and $W_1(x) = -k_1^2\alpha_2(x)$.

The analytical solution of Eq. (2) with variable coefficients can be likewise expressed as Eq. (12). In Fig. 2, we take the variable coefficient $\eta_1(t)$ as sine function. It is obvious that the soliton solution is periodic and $\sigma_2(t)$ is related to the amplitude.

When $W_2(t) = at\,\mathrm{e}^{-t^2}$, $\eta_1(t) = b\,\mathrm{e}^{-t^2}$, $\sigma_2(t) = c\,\mathrm{e}^{-t^2}$, it can be seen that a and b have effects on the amplitude and phase shift of soliton near $t = 0$, respectively. The amplitude of soliton in $t \geq 0$ is directly proportional to c, and the other part is inversely (see Fig. 3).

3 Analysis of numerical solutions

To study the effect of fourth-order nonlinear dispersion numerically, we consider the generalized case with con-

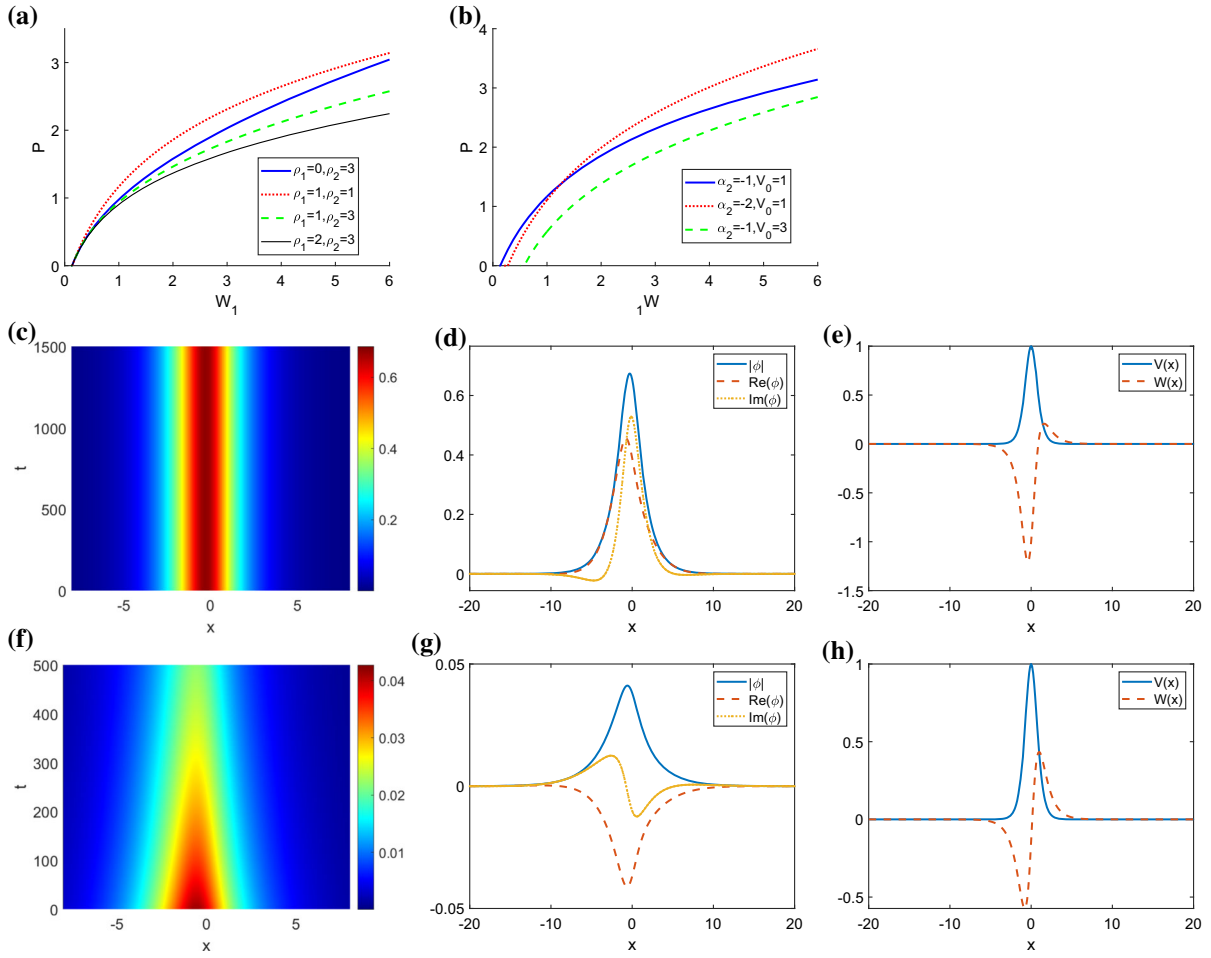

Fig. 4 Parameters are chosen as: $\alpha_1 = 1$, $\beta_1 = 1$, $\beta_2 = 1$, $\sigma_1 = 0.05$, $\sigma_2 = 0$, $W_0 = 1$, with **a** $\alpha_2 = -1$, $V_0 = 1$, with **b** $\rho_1 = 1$, $\rho_2 = 1$, with **c–e** $\alpha_2 = -1$, $\rho_1 = 1$, $\rho_2 = 1$, $V_0 = 1$, $W_1 = 1$, with **f–h** $\alpha_2 = -1$, $\rho_1 = 1$, $\rho_2 = 1$, $V_0 = 1$, $W_1 = 0.14$

stant coefficients and complex potentials

$$iu_t + (\alpha_1 + i\alpha_2)u_{xx} + (\beta_1 + i\beta_2)|u|^2u + [V(x) + iW(x)]u + (\sigma_1 + i\sigma_2)u_{xxxx} + (\rho_1 + i\rho_2)u|u|^4 = 0, \tag{15}$$

where $\alpha_i, \beta_i, \sigma_i$ and ρ_i $(i = 1, 2)$ are all real parameters. We focus on the stationary solutions of Eq. (15) in the form:

$$u(x,t) = \phi(x)e^{i\mu t}, \tag{16}$$

where μ is a real propagation constant.

Substituting it into Eq. (15), we can obtain the complex localized field-amplitude function $\phi(x)$ that satisfies the ordinary differential equation:

$$\left[(\alpha_1 + i\alpha_2)\frac{d^2}{dx^2} + (\beta_1 + i\beta_2)|\phi|^2 + V(x) + iW(x) + (\sigma_1 + i\sigma_2)\frac{d^4}{dx^4} + (\rho_1 + i\rho_2)|\phi|^4\right]\phi = \mu\phi. \tag{17}$$

In our numerical simulations, spatial differential and the integration in time are carried out by the modified squared-operator method and the pseudospectral method, respectively [47]. In the following, we study Eq. (15) under the role of the near $\mathcal{PT}$-symmetric Scarf-II and δ-signum potentials and find the stationary nonlinear modes of Eq. (15).

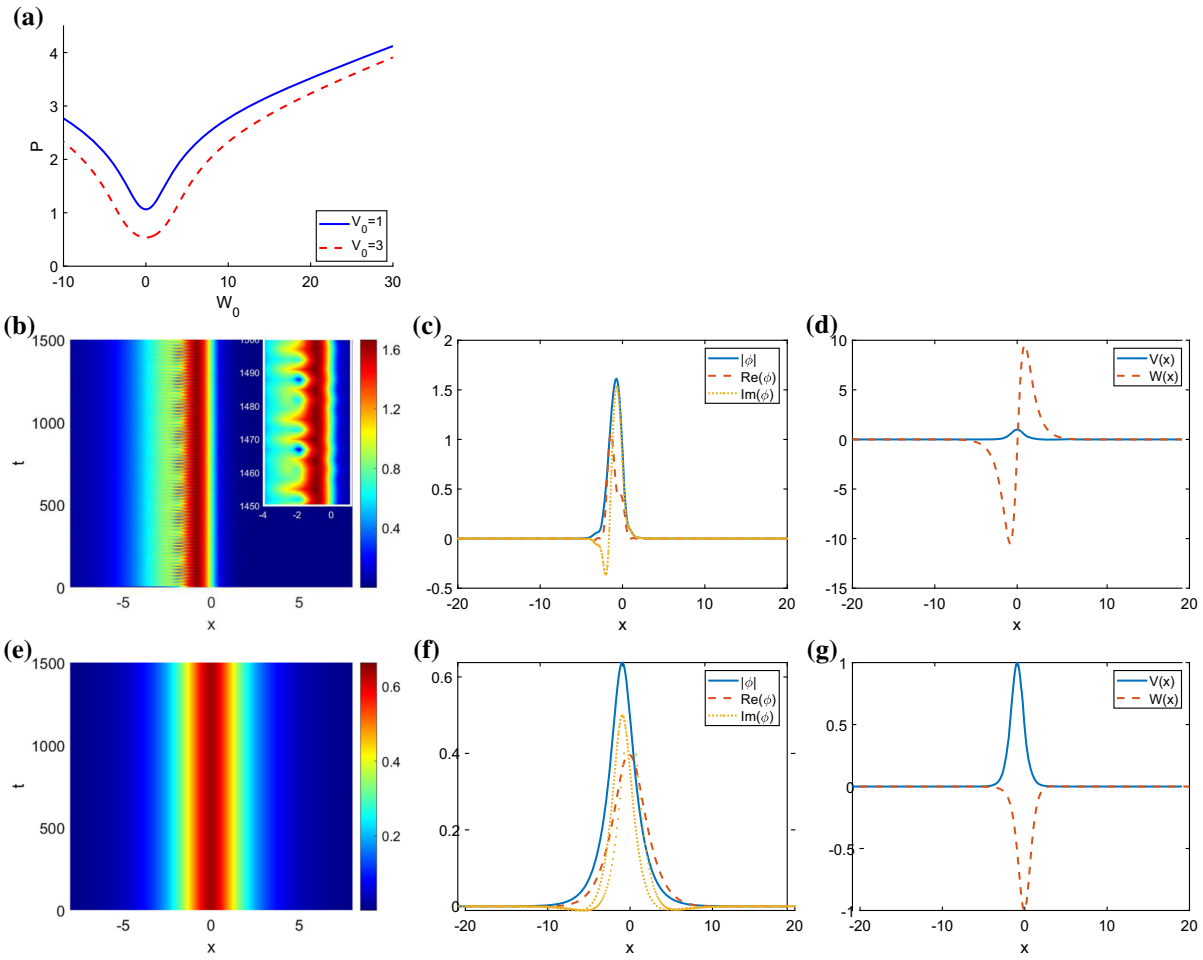

Fig. 5 Parameters are chosen as: Parameters are chosen as: $\alpha_1 = 1$, $\alpha_2 = -1$, $\beta_1 = 1$, $\beta_2 = 1$, $\rho_1 = 1$, $\rho_2 = 1$, $\sigma_1 = 0.05$, $\sigma_2 = 0$, $W_1 = 1$, with **b**–**d** $V_0 = 1$, $W_0 = 20$, with **e**–**g** $V_0 = 1$, $W_0 = 0.1$

3.1 Nonlinear modes with the near $\mathcal{PT}$-symmetric Scarf-II potential

The $\mathcal{PT}$-symmetric complex potential $V(x) + iW(x)$ has the features that $V(x) = V(-x)$ and $W(-x) = -W(x)$ [3]. Because of the appearance of complex coefficients, Eq. (2) is not $\mathcal{PT}$-symmetric. The near $\mathcal{PT}$-symmetric potentials are considered [10]. We initiate our analysis by introducing the following near $\mathcal{PT}$-symmetric Scarf-II potential

$$\begin{aligned} V(x) &= V_0 \,\mathrm{sech}^2(x), \\ W(x) &= W_0 \,\mathrm{sech}(x)\tanh(x) - W_1 \,\mathrm{sech}^2(x). \end{aligned} \tag{18}$$

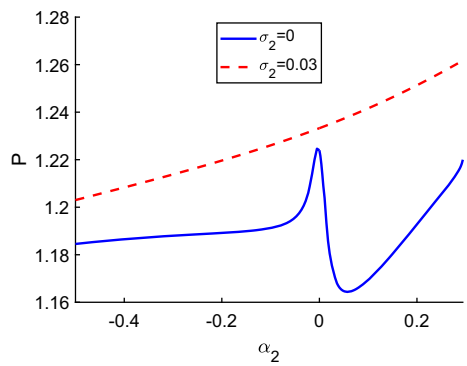

Fig. 6 Parameters are chosen as: $\alpha_1 = 1$, $\beta_1 = 1$, $\beta_2 = 1$, $\rho_1 = 1$, $\rho_2 = 1$, $\sigma_1 = 0.05$, $V_0 = 1$, $W_0 = 1$, $W_1 = 1$

After setting some coefficients, we study the effects of other variables on the iterative image. The power of nonlinear mode is defined as $P = \int_{-\infty}^{+\infty} |\phi(x,t)|^2 dx$. The relationship between ρ_1, ρ_2, α_2, V_0, W_1 and P is shown in Fig. 4a and b, in which the horizontal coordinate is $W_1 \in (0, 6)$. When other parameters are specified, W_1 and P are positively correlated, while ρ_1, ρ_2 and P are negatively correlated (see Fig. 4a). What's more, when α_2 is different in two cases, we can make them have the same power by adjusting W_1 (see Fig. 4b).

In addition, when $W_1 = 0$, the near $\mathcal{PT}$-symmetric potential (18) is just the conventional $\mathcal{PT}$-symmetric Scarf-II potential. With the value of W_1 decreasing, the solution will be unstable and become attenuation by the propagation of soliton. Now, we consider the evolution of soliton solutions via Eq. (16). In our numerical simulations, the 5% initial random noise is added to simulate the wave transmission. With the given parameters, Fig. 4c displays a stable nonlinear mode. If the value of W_1 is decreased, the mode will become unstable. This is to say a little change in the gain–loss distributions can make the nonlinear mode unstable when W_1 is sufficiently small (see Fig. 4f).

Furthermore, it will get close to $\mathcal{PT}$-symmetric Scarf-II potential by increasing the value of W_0. In this case, the relationship between P and W_0 is illustrated in Fig. 5a. If the initial value of $W_0 = 20W_1$, then the amplitude of nonlinear mode is periodically oscillating and it experiences more than 2 periods within $1450 \le t \le 1500$ (see Fig. 5b). This means the growth of W_0 can also change the stability of soliton with near $\mathcal{PT}$-symmetric Scarf-II potential.

When other coefficients are fixed, we change W_0 to get different potentials. Let $W_0 = 0.1$, and W approximates an even function of x. Moreover, the soliton is stable and symmetric approximately (see Fig. 5e and f). If we further increase W_0 to 20, then W is close to an odd function of x. What's more, the soliton is stable and asymmetric (see Fig. 5b and c), which indicates that we can get stable soliton with near $\mathcal{PT}$-symmetric Scarf-II potential by increasing the value of W_0.

In particular, for some small values of W_0, the soliton in cubic GLE is usually stable with $\alpha_2 \le 0$ and $\beta_2 \ge 0$, beyond which the soliton immediately becomes extremely unstable [10]. So we investigate the relationship between P and α_2 with the fourth-order magnetic interactions σ_2 (see Fig. 6). When $\alpha_2 > 0$ and $\sigma_2 = 0$, P of the nonlinear mode changes suddenly near $t = 0$. If we fix $\sigma_2 = 0.03$, the curve about P and α_2 of nonlinear mode will become smooth. Thus, the power of the nonlinear mode can be transformed by changing σ_2.

3.2 Nonlinear modes with the near $\mathcal{PT}$-symmetric δ-signum potential

Next, we introduce the near $\mathcal{PT}$-symmetric δ-signum potential

$$\begin{aligned} V(x) &= 2V_0\delta(x), \\ W(x) &= W_0\,\mathrm{sgn}(x)e^{-V_0|x|} - W_1\delta(x), \end{aligned} \tag{19}$$

to carry on our analysis, which plays a significant role in such fields as quantum physics, optics and Bose–Einstein condensates [48,49].

The limit of the following Gaussian function can be used to express the δ function

$$\begin{aligned} \delta(x) &= \lim_{a\to 0^+} g(x;a), \\ g(x;a) &= \frac{\exp(-x^2/a^2)}{a\sqrt{\pi}}, \end{aligned} \tag{20}$$

and thus, we can use the Gaussian function $g(x;a)$ with very small parameter a to approximate the δ function [48]. In order to facilitate calculations, without loss of generality, we choose $a = 0.01$ in this paper.

As shown in Fig. 7a and b, the horizontal coordinates are $W_1 \in (0, 6)$. W_1 is directly proportional to P. β_2, ρ_1, ρ_2 are inversely proportional to P. And when W_1 is sufficiently small, the peakon solution is becoming unstable. Results of these numerical simulations are given in Fig. 7c and e.

When the horizontal coordinates are $W_0 \in (-5, 20)$, Fig. 8a shows the power of peakon solutions. When $W_0 = 0$, P takes the minimum value. Considering W_0 as large as possible, the evolution of peakon is similar to the case under the near $\mathcal{PT}$-symmetric Scarf-II potential and it experiences more than 5 periods within $1450 \le t \le 1500$ (see Fig. 8b).

Based on the above results, we consider the effect of β_2 and ρ_2. It is easy to show that β_2 and ρ_2 are inversely proportional to P. The two stable peakon solutions are illustrated in Fig. 9c and e. It can be seen that β_2 are related to the morphology of peakons by changing the width of nonlinear mode.

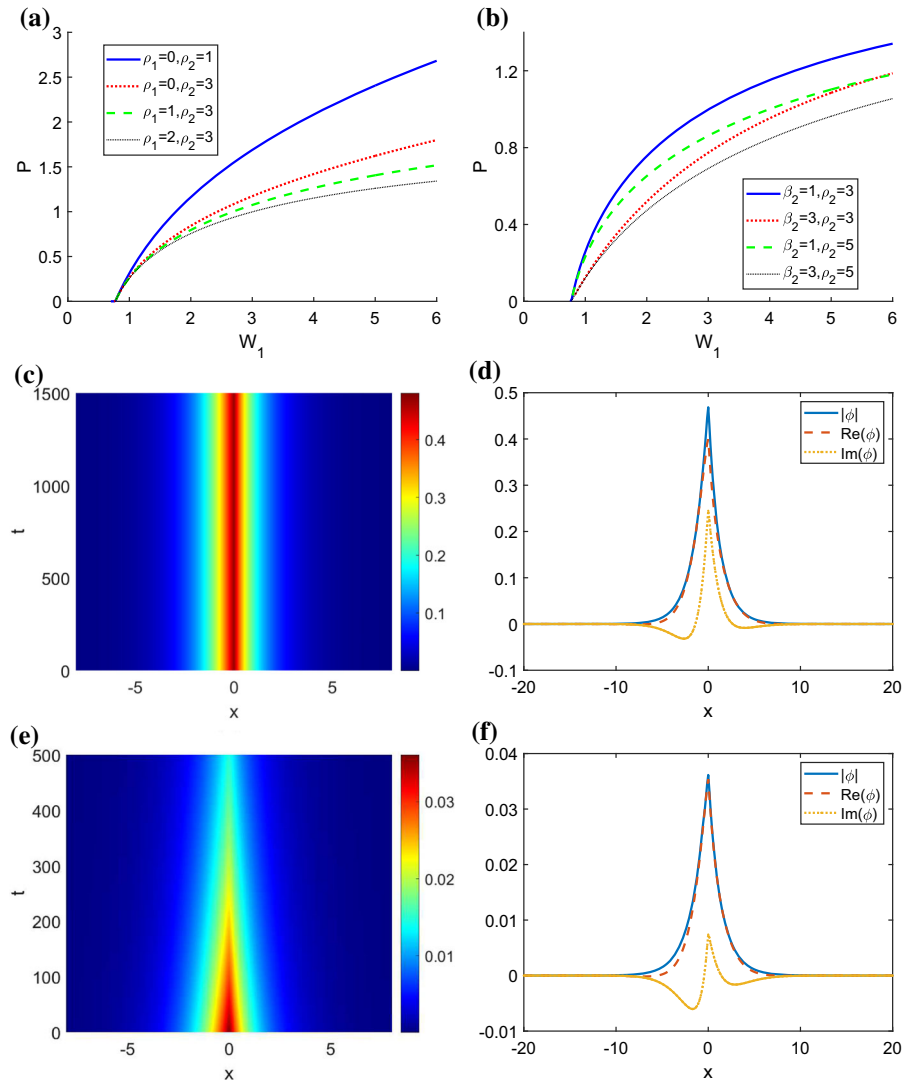

Fig. 7 Parameters are chosen as: $\alpha_1 = 1$, $\alpha_2 = -1$, $\beta_1 = 1$, $\sigma_1 = \sigma_2 = 0$, $V_0 = 1$, $W_0 = 1$, with **a** $\beta_2 = 1$, with **b** $\rho_1 = 2$, with **c**, **d** $\beta_2 = 1$, $\rho_1 = 0$, $\rho_2 = 1$, $W_1 = 1$, with **e**, **f** $\beta_2 = 1$, $\rho_1 = 0$, $\rho_2 = 1$, $W_1 = 0.77$

3.3 Generalized model and excitations of solitons

In this section, we consider excitations of the above-mentioned solitons in Eq. (15) via adiabatical change of system parameters. We restrict our interests in the following nonlinear modes with the near $\mathcal{PT}$-symmetric potentials (18) (19) and complex coefficients of Eq. (15)

$$\begin{aligned} & iu_t + [\alpha_1 + i\alpha_2(t)]\, u_{xx} \\ & \quad + [\beta_1 + i\beta_2]\, |u|^2 u + [V(x) + iW(x,t)]u \\ & \quad + [\sigma_1 + i\sigma_2]\, u_{xxxx} + [\rho_1 + i\rho_2]\, u|u|^4 = 0. \end{aligned} \tag{21}$$

In order to modulate the system parameters smoothly, we consider the following "switch-on" function:

$$\epsilon(t) = \begin{cases} \epsilon_1, & t = 0, \\ \dfrac{1}{2}(\epsilon_2 - \epsilon_1)\left[1 + \sin\left(\dfrac{\pi t}{500} - \dfrac{\pi}{2}\right)\right] + \epsilon_1, & 0 < t < 500, \\ \epsilon_2, & 500 \le t \le 1500, \end{cases} \tag{22}$$

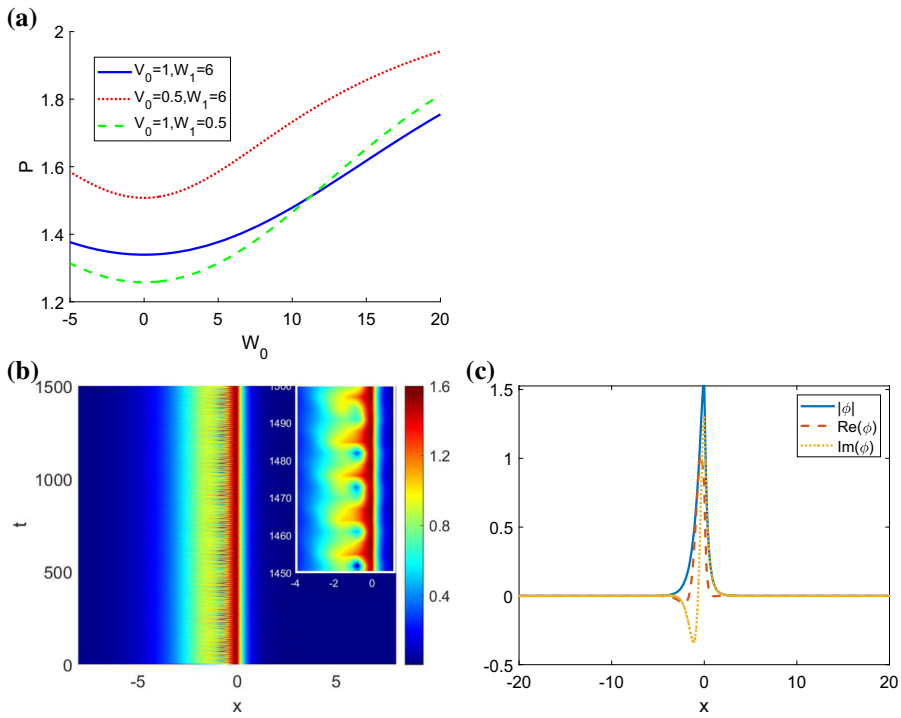

Fig. 8 Parameters are chosen as: $\alpha_1 = 1$, $\alpha_2 = -1$, $\beta_1 = 1$, $\beta_2 = 1$, $\rho_1 = 2$, $\rho_2 = 3$, $\sigma_1 = \sigma_2 = 0$, with **b**, **c** $V_0 = 1$, $W_0 = 20$, $W_1 = 6$

where $\epsilon_{1,2}$, respectively, represent the real initial-state and final-state parameters and generate $\alpha_2(t)$, $W_0(t)$, $W_1(t)$ by $\epsilon(t)$. Under the synchronous modulation of system parameters, the excitation stage and the propagation stage can be described by Eqs. (21), (22). During the excitation stage ($0 < t < 500$), system parameters change slowly from ϵ_1 to ϵ_2, and the initial state corresponding to ϵ_1 will be adiabatically driven to the new state corresponding to ϵ_2; during the propagation stage ($500 \leq t \leq 1500$), system parameters are maintained at ϵ_2, and the excited nonlinear mode will propagate in the final system. It should be noted that some system parameters can be constants [e.g., $W_0(x, t) = \epsilon(t)$ = const.], if we set the "switch-on" function $\epsilon(t)$ for $\epsilon_1 = \epsilon_2$ [50].

We first execute a two-parameter excitation of the soliton with the near $\mathcal{PT}$-symmetric Scarf-II potential. Figure 10 shows that the excitation of the nonlinear mode is stable with a lower amplitude with the change of W_0 and W_1, due to both the final state and initial state are stable.

Because the solutions in Fig. 6 cannot be obtained directly when $\alpha_2 \geq 0$, we consider the case in this section. As can be seen, Fig. 11 shows a stable soliton solution.

Finally, we consider the near $\mathcal{PT}$-symmetric δ-signum potential. We execute a single-parameter excitation of the peakon controlled by Eq. (21) via the initial condition determined. In Fig. 12, it can be seen that if $W_{01} = 1$ and $W_{11} = 20$, then the morphology of stable mode will change.

4 Conclusions

In conclusion, we study the dynamic behavior and stability of nonlinear modes in the fourth-order generalized GLE with near $\mathcal{PT}$-symmetric potentials.

Firstly, we get the bilinear form of Eq. (2) by Hirota method. When the coefficients are constant and variable, analytical solutions and images of solitary wave solutions are obtained, respectively. In constant coefficients, the velocity and direction of the solitonic propagation phase will be changed if we choose different values of η_1 (see Fig. 1). In various coefficients, the intensity of soliton is related to $\sigma_2(t)$ and the soliton solution is periodic when the variable coefficient $\eta_1(t)$ is sine function (see Fig. 2).

Secondly, we separately study the model of Eq. (15) with two novel categories of near $\mathcal{PT}$-symmetric Scarf-II and δ-signum potentials and get several stable soli-

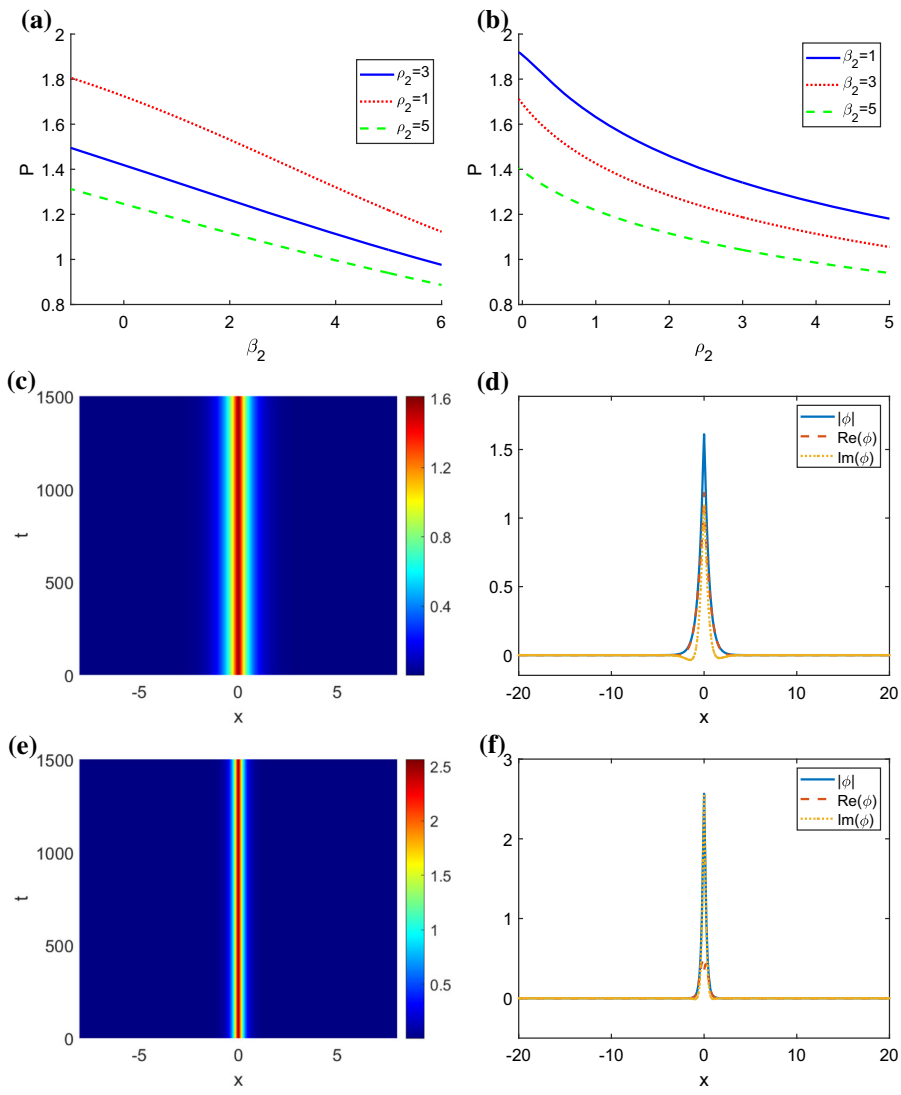

Fig. 9 Parameters are chosen as: $\alpha_1 = 1$, $\alpha_2 = -1$, $\beta_1 = 1$, $\rho_1 = 2$, $\sigma_1 = \sigma_2 = 0$, $V_0 = 1$, $W_0 = 1$, $W_1 = 6$, with **a** $\rho_2 = 3$, with **b** $\beta_2 = 1$, with **c**, **d** $\beta_2 = -1$, $\rho_2 = 3$, with **e**, **f** $\beta_2 = 1$, $\rho_2 = 0$

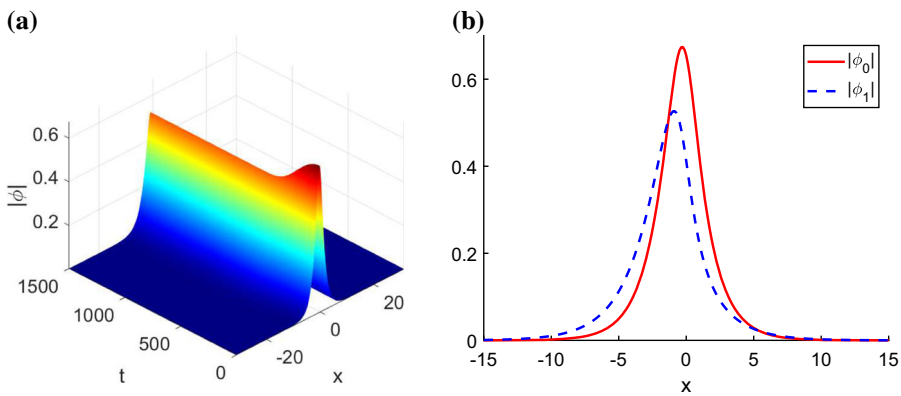

Fig. 10 Parameters are chosen as: $\alpha_1 = 1$, $\alpha_2 = -1$, $\beta_1 = 1$, $\beta_2 = 1$, $\rho_1 = 1$, $\rho_2 = 1$, $\sigma_1 = 0.05$, $\sigma_2 = 0$, $V_0 = 1$, $W_{01} = 1$, $W_{02} = 2$, $W_{11} = 1$, $W_{12} = 0.14$

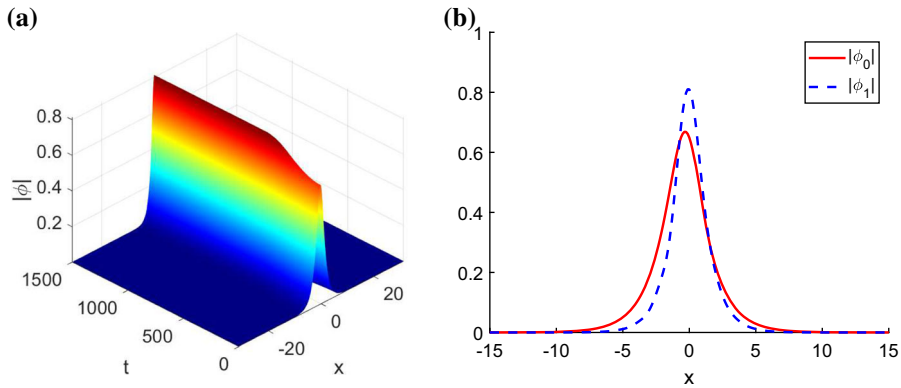

Fig. 11 Parameters are chosen as: $\alpha_1 = 1, \beta_1 = 1, \beta_2 = 1, \rho_1 = 1, \rho_2 = 1, \sigma_1 = 0.05, \sigma_2 = 0.03, V_0 = 1, W_0 = 1, W_1 = 1, \alpha_{21} = -1, \alpha_{22} = 0$

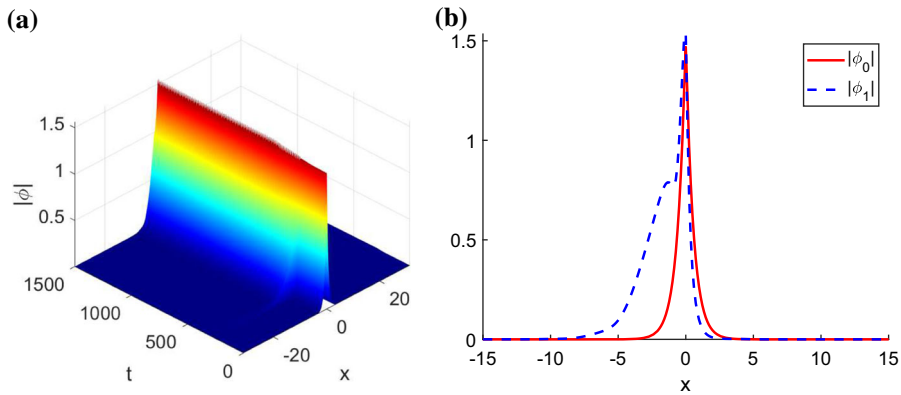

Fig. 12 Parameters are chosen as: $\alpha_1 = 1, \alpha_2 = -1, \beta_1 = 1, \beta_2 = 1, \rho_1 = 2, \rho_2 = 3, \sigma_1 = \sigma_2 = 0, V_0 = 1, W_1 = 6, W_{01} = 1, W_{02} = 20$

ton and peakon solutions. Besides, the relationships between system coefficients and the power of nonlinear modes are investigated. Roughly speaking, W_1 and P are positively correlated, while ρ_1, ρ_2 and P are negatively correlated (see Figs. 4a and 7a). When $W_0 = 0$, the power of nonlinear modes takes the minimum value (see Figs. 5a and 8a). In particular, with the near $\mathcal{PT}$-symmetric Scarf-II potential, if the initial value of $W_0 = 20W_1$, W is close to an odd function of x and the amplitude of nonlinear mode is periodically oscillating (see Fig. 5b and d). Let $W_0 = 0.1$, then W approximates to an even function of x and the soliton is stable and symmetric approximately (see Fig. 5e and g). With the near $\mathcal{PT}$-symmetric δ-signum potential, β_2 is related to the morphology of peakons by changing the width of nonlinear mode and it is inversely proportional to the power of the peakon (see Fig. 9).

Finally, we analyze the excitations of nonlinear modes and get some stable cases that have not been acquired in the second part. It can be seen that the morphology of the stable mode is changed when we execute a single-parameter excitation of the peakon (see Figs. 11 and 12).

Acknowledgements We express our sincere thanks to the editor, referees and all the members of our discussion group for their valuable comments. This work was supported by the National Training Program of Innovation (Grant numbers 202210019045). The funding body plays an important role in the design of the study, in analysis, calculation, and in writing of the manuscript.

Funding This work was supported by the National Training Program of Innovation (Grant numbers 202210019045). The funding body plays an important role in the design of the study, in analysis, calculation, and in writing of the manuscript.

Data availability The authors declare that the manuscript has no associated data.

Declarations

Conflict of interest The authors declare that they have no conflict of interest.

References

1. Ablowitz, M.J., Segur, H.: Solitons and the Inverse Scattering Transform. SIAM, Philadelphia (1981)
2. Ablowitz, M.J., Clarkson, P.A.: Solitons. Nonlinear Evolution Equations and Inverse Scattering. Cambridge University Press, Cambridge (1991)
3. Musslimani, Z., Makris, K.G., El-Ganainy, R., Christodoulides, D.N.: Optical solitons in $\mathcal{PT}$ periodic potentials. Phys. Rev. Lett. **100**, 030402 (2008)
4. Konotop, V.V., Yang, J., Zezyulin, D.A.: Nonlinear waves in $\mathcal{PT}$-symmetric systems. Rev. Mod. Phys. **88**, 035002 (2016)
5. Kartashov, Y.V., Astrakharchik, G.E., Malomed, B.A., Torner, L.: Frontiers in multidimensional self-trapping of nonlinear fields and matter. Nature Rev. Phys. **1**, 185–197 (2019)
6. Mihalache, D.: Localized structures in optical and matter-wave media: a selection of recent studies. Rom. Rep. Phys. **73**, 403 (2021)
7. Nozaki, K., Bekki, N.: Pattern Selection and Spatiotemporal Transition to Chaos in the Ginzburg-Landau Equation. Phys. Rev. Lett. **12**, 2154 (1983)
8. Haken, H.: Generalized Ginzburg-Landau equations for phase transitionlike phenomena in lasers, nonlinear optics, hydrodynamics and chemical reactions. Z. Phys. B **21**, 105 (1975)
9. Aranson, I.S., Kramer, L.: The world of the complex Ginzburg-Landau equation. Rev. Mod. Phys. **74**, 99–143 (2002)
10. Chen Y., Yan Z., Liu W.: Impact of near-$\mathcal{PT}$ symmetry on exciting solitons and interactions based on a complex Ginzburg-Landau model. Opt. Express, 2625 (2018)
11. Ipsen, M., Kramer, L., Sørensen, P.G.: Amplitude equations for description of chemical reaction-diffusion systems. Phys. Rep. **337**, 193–235 (2000)
12. van Hecke, M.: Coherent and incoherent structures in systems described by the 1D CGLE: experiments and identification. Phys. D **174**, 134–151 (2003)
13. Akhmediev, N., Ankiewicz, A., Soto-Crespo, J.: Multisoliton solutions of the complex Ginzburg-Landau equation. Phys. Rev. Lett. **79**, 4047 (1997)
14. Akhmediev, N., Soto-Crespo, J.M.: Exploding solitons and Shil'nikov's theorem. Phys. Lett. A **317**, 287–292 (2003)
15. Skarka, V., Aleksic, N., Leblond, H., Malomed, B., Mihalache, D.: Varieties of stable vortical solitons in Ginzburg-Landau media with radially inhomogeneous losses. Phys. Rev. Lett. **105**, 213901 (2010)
16. He, Y., Mihalache, D.: Lattice solitons in optical media described by the complex Ginzburg-Landau model with $\mathcal{PT}$-symmetric periodic potentials. Phys. Rev. A **87**, 013812 (2013)
17. Soto-Crespo, J.M., Akhmediev, N., Chiang, K.S.: Simultaneous existence of a multiplicity of stable and unstable solitons in dissipative systems. Phys. Lett. A **291**, 115–123 (2001)
18. Zhang, H.Q., Tian, B., Meng, X.H., Lü, X., Liu, W.J.: Conservation laws, soliton solutions and modulational instability for the higher-order dispersive nonlinear Schrödinger equation. Eur. Phys. J. B **72**, 233–239 (2009)
19. Akhmediev, N., Soto-Crespo, J.M., Town, G.: Pulsating solitons, chaotic solitons, period doubling, and pulse coexistence in mode-locked lasers: Complex Ginzburg-Landau equation approach. Phys. Rev. E **63**, 056602 (2001)
20. Zong, F.D., Dai, C.Q., Yang, Q., Zhang, J.F.: Soliton solutions for variable coefficient nonlinear Schrödinger equation for optical fiber and their application. Acta Phys. Sin. **55**, 3805 (2006)
21. Liu, W.J., Tian, B., Jiang, Y., Sun, K., Wang, P., Li, M., Qu, Q.X.: Soliton solutions and Bäcklund transformation for the complex Ginzburg-Landau equation. Appl. Math. Comput. **2017**, 4369–4376 (2011)
22. Bender, C.M., Boettcher, S.: Real spectra in non-Hermitian Hamiltonians having $\mathcal{PT}$ symmetry. Phys. Rev. Lett. **80**, 5243 (1998)
23. Bender, C.M., Brody, D.C., Jones, H.F.: Must a Hamiltonian be Hermitian? Am. J. Phys **71**, 1095–1102 (2003)
24. Bender, C.M.: Making sense of non-Hermitian Hamiltonians. Rep. Prog. Phys. **70**, 947–1018 (2007)
25. Guo, A., Salamo, G., Duchesne, D., Morandotti, R., Volatier-Ravat, M., Aimez, V., Siviloglou, G., Christodoulides, D.: Observation of $\mathcal{PT}$-symmetry breaking in complex optical potentials. Phys. Rev. Lett. **103**, 093902 (2009)
26. Rüter, C.E., Makris, K.G., El-Ganainy, R., Christodoulides, D.N., Segev, M., Kip, D.: Observation of parity-time symmetry in optics. Nat. Phys. **6**, 192–195 (2010)
27. Regensburger, A., Bersch, C., Miri, M.A., Onishchukov, G., Christodoulides, D.N., Peschel, U.: Parity-time synthetic photonic lattices. Nature **488**, 167–171 (2012)
28. Castaldi, G., Savoia, S., Galdi, V., Alù, A., Engheta, N.: $\mathcal{PT}$ metamaterials via complex-coordinate transformation optics. Phys. Rev. Lett. **110**, 173901 (2013)
29. Regensburger, A., Miri, M.A., Bersch, C., Näger, J., Onishchukov, G., Christodoulides, D.N., Peschel, U.: Observation of defect states in $\mathcal{PT}$-symmetric optical lattices. Phys. Rev. Lett. **110**, 223902 (2013)
30. Peng, B., Özdemir, S.K., Lei, F., Monifi, F., Gianfreda, M., Long, G.L., Fan, S., Nori, F., Bender, C.M., Yang, L.: Parity-time-symmetric whispering-gallery microcavities. Nat. Phys. **10**, 394–398 (2014)
31. Zyablovsky, A.A., Vinogradov, A.P., Pukhov, A.A., Dorofeenko, A.V., Lisyansky, A.A.: $\mathcal{PT}$-symmetry in optics. Phys. Usp. **57**, 1063 (2014)
32. Chen, P.Y., Jung, J.: $\mathcal{PT}$ Symmetry and Singularity-Enhanced Sensing Based on Photoexcited Graphene Metasurfaces. Phys. Rev. Appl **5**, 064018 (2016)
33. Takata, K., Notomi, M.: $\mathcal{PT}$-Symmetric Coupled-Resonator Waveguide Based on Buried Heterostructure Nanocavities. Phys. Rev. Appl **7**, 054023 (2017)
34. Lumer, Y., Plotnik, Y., Rechtsman, M.C., Segev, M.: Nonlinearly induced $\mathcal{PT}$ transition in photonic systems. Phys. Rev. Lett. **111**, 263901 (2013)
35. Chen, H., Hu, S.: The asymmetric solitons in two-dimensional parity-time symmetric potentials. Phys. Lett. A **380**, 162 (2016)
36. Kominis, Y.: Soliton dynamics in symmetric and non-symmetric complex potentials. Opt. Commun. **334**, 265–272 (2015)
37. Kominis, Y.: Dynamic power balance for nonlinear waves in unbalanced gain and loss landscapes. Phys. Rev. A **92**, 063849 (2015)

38. Tsoy, E.N., Allayarov, I.M., Abdullaev, F.K.: Stable localized modes in asymmetric waveguides with gain and loss. Opt. Lett. **39**, 4215–4218 (2014)
39. Yan, Z., Chen, Y., Wen, Z.: On stable solitons and interactions of the generalized Gross-Pitaevskii equation with $\mathcal{PT}$-and non-$mathcal PT$-symmetric potentials. Chaos **26**, 083109 (2016)
40. Konotop, V.V., Zezyulin, D.A.: Families of stationary modes in complex potentials. Opt. Lett. **39**, 5535–5538 (2014)
41. Nixon, S.D., Yang, J.: Bifurcation of soliton families from linear modes in non-$\mathcal{PT}$-symmetric complex potentials. Stud. Appl. Math. **136**, 459–483 (2016)
42. Yang, J., Nixon, S.: Stability of soliton families in nonlinear schrödinger equations with non-parity-time-symmetric complex potentials. Phys. Lett. A **380**, 3803–3809 (2016)
43. Kominis, Y., Cuevas-Maraver, J., Kevrekidis, P.G., Frantzeskakis, D.J., Bountis, A.: Continuous families of solitary waves in non-symmetric complex potentials: a Melnikov theory approach. Chaos Solitons Fractals **118**, 222–233 (2019)
44. Midya, B., Roychoudhury, R.: Nonlinear localized modes in $\mathcal{PT}$-symmetric Rosen-Morse potential wells. Phys. Lett. A **87**, 045803 (2013)
45. Hari, K., Manikandan, K., Sankaranarayanan, R.: Dissipative optical solitons in asymmetric Rosen-Morse potential. Phys. Lett. A **384**, 126104 (2020)
46. Hirota, R.: The Direct Method in Soliton Theory. Springer, Berlin (1980)
47. Yang, J.: Nonlinear Waves in Integrable and Nonintegrable Systems. SIAM, Philadelphia (2010)
48. Chen, Y., Yan, Z., Mihalache, D.: Stable flat-top solitons and peakons in the $\mathcal{PT}$-symmetric δ-signum potentials and nonlinear media. Chaos **29**, 083108 (2019)
49. Cartarius, H., Wunner, G.: Model of a $\mathcal{PT}$-symmetric Bose-Einstein condensate in a δ-function double-well potential. Phys. Rev. A **86**, 013612 (2012)
50. Shen, Y.J., Wen, Z.C., Yan, Z.Y., Hang, C.: Effect of symmetry on nonlinear waves for three-wave interaction models in the quadratic nonlinear media. Chaos **28**, 043104 (2018)